Supplementary Information

Kai-Cheng Zhang[1*] and Lin-Yuan Cheng[1]
[1] *School of Physical Science and Technology, Bohai University, Jinzhou 121013, China*

Chen Shen[2]
[2] *Institute of Materials Science, Technical University of Darmstadt, Alarich-Weiss-Str. 2, 64287 Darmstadt, Germany*

Yong-Feng Li[3,4]
[3] *School of Science, Inner Mongolia University of Science and Technology, Baotou 014010, China*
[4] *Key laboratory of Integrated Exploitation of Bayan Obo Multi-Metal Resources, Inner Mongolia University of Science and Technology, Baotou 014010, China*

Yong Liu[5]
[5] *State Key Laboratory of Metastable Materials Science & Technology and College of Science, Yanshan University, Qinhuangdao, Hebei 066004, China*

Yan Zhu[6]
[6] *Department of Physics, Nanjing University of Aeronautics and Astronautics, Nanjing 210016, China*

(Dated: May 14, 2021)

*kczhang@yeah.net

TABLE S1. The optimized lattice constants and bond lengths for layered and bulk $PdSe_2$.

	a	b	$d_{\mathrm{Pd-Se}}$	$d_{\mathrm{Se-Se}}$
1L	5.740	5.913	2.450	2.417
2L	5.767	5.925	2.455	2.419
3L	5.770	5.927	2.460	2.419
4L	5.773	5.929	2.466	2.418
5L	5.774	5.929	2.467	2.419
6L	5.776	5.931	2.472	2.424
Bulk	5.783	5.934	2.491	2.439

TABLE S2. The frequencies (THz) of infrared Raman modes B_{2u}^2, B_{1u}^1, and A_u^3 for layered and bulk $PdSe_2$.

	B_{2u}^2	B_{1u}^1	A_u^3
2L	0.466	0.293	0.370
3L	0.463	0.342	0.419
4L	0.514	0.345	0.438
Bulk	1.041	0.671	0.939

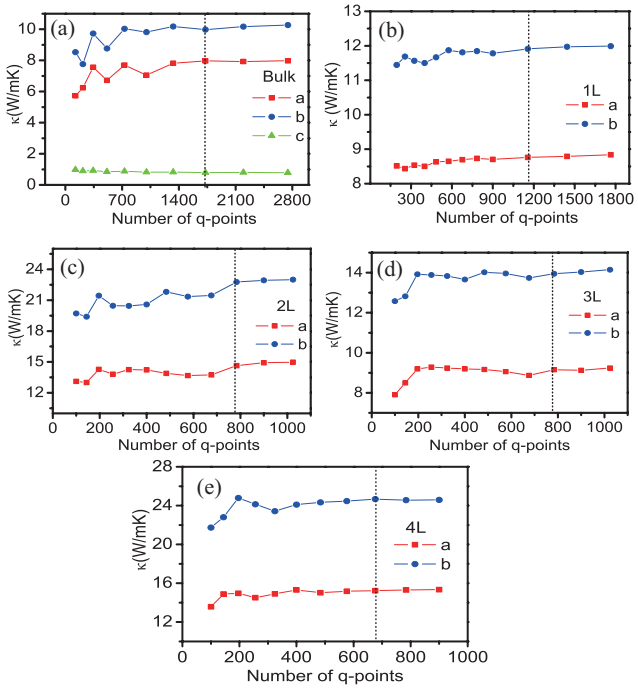

FIG. S1. Convergence tests of q points used in the ShengBTE calculations for the bulk (a) 1L (b), 2L (c), 3L (d) and 4L (e) $PdSe_2$. The dotted lines mark the convergence of thermal conductivity.

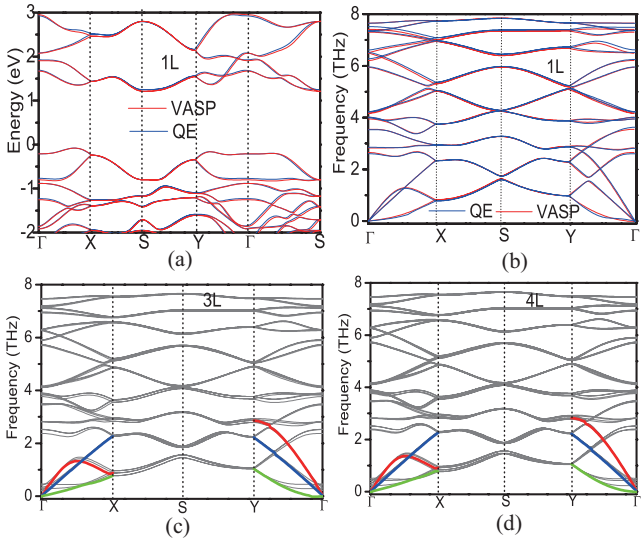

FIG. S2. The electronic (a) and phonon (b) band structures of 1L $PdSe_2$ calculated by VASP (red line) and QE (blue line) codes. Phonon dispersion for 3L (c) and 4L (d) $PdSe_2$. The red, blue and green curves represent LA, TA and ZA modes.

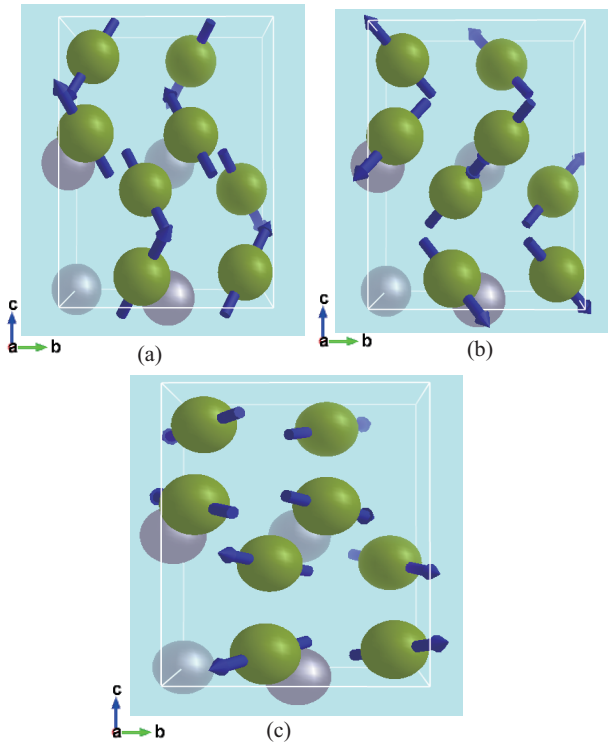

FIG. S3. Atom vibrations of Raman active modes A_g^1(a), A_g^3(b) and B_{1g}^2(c) for bulk $PdSe_2$.

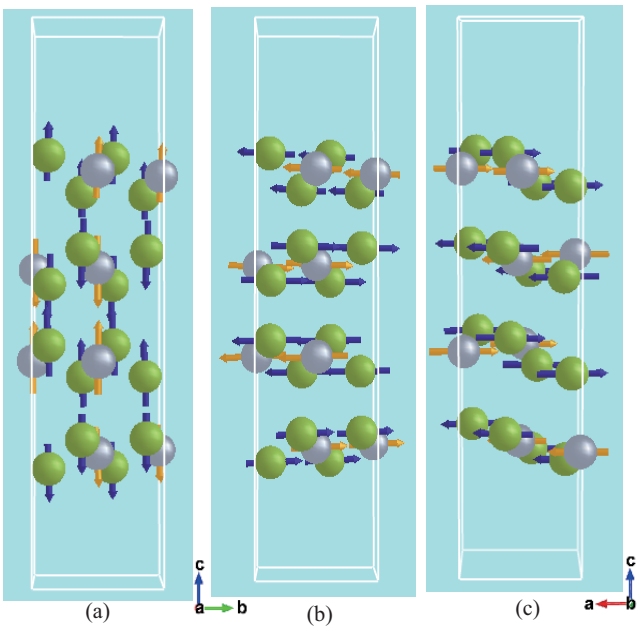

FIG. S4. Atom vibrations of low-frequency optical modes B^2_{2u} (a), B^1_{1u}(b) and A^3_u(c) for 4L $PdSe_2$. Among them, B^2_{2u} and B^1_{1u} are infrared Raman active.

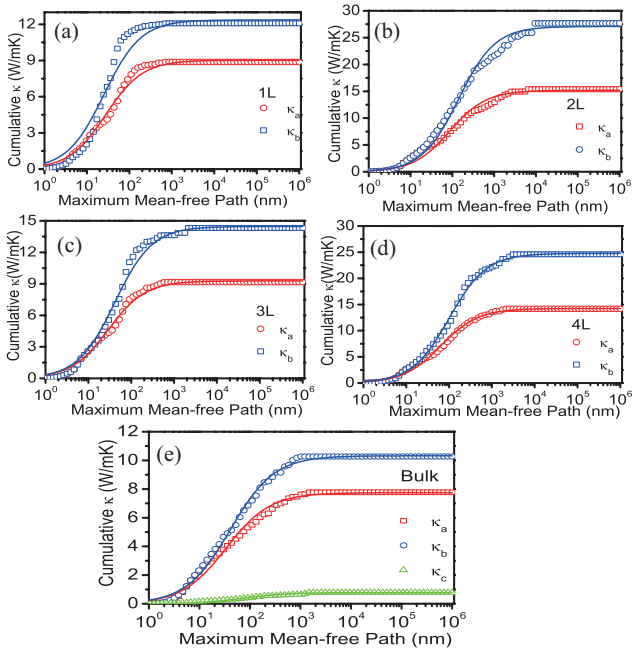

FIG. S5. The cumulative thermal conductivities versus maximum mean-free path for 1L (a), 2L (b), 3L (c), 4L (d) and bulk (e) $PdSe_2$. The lines are the fittings with the function $\kappa = \kappa_0/(1+\ell_0/\ell)$, where ℓ_0 is the representative mean-free path (rMFP) of phonon.

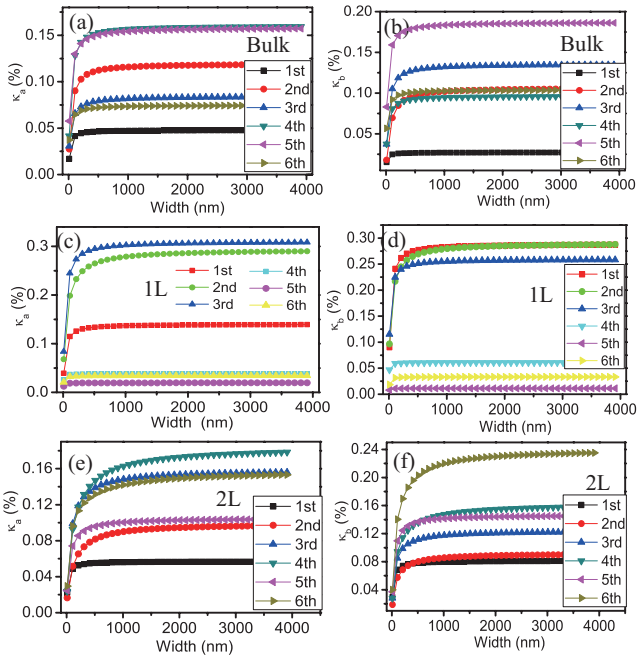

FIG. S6. Mode-resolved thermal contribution versus the width of nanowires along the a and b axes for bulk (a)-(b), 1L (c)-(d) and 2L (e)-(f) $PdSe_2$. The contributions (in %)from six lowest modes are plotted.

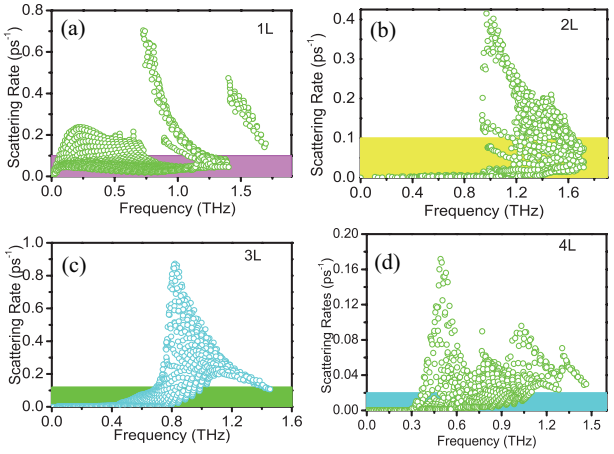

FIG. S7. Frequency-dependent scattering rates of ZA mode for 1L (a), 2L (b), 3L (c) and 4L (d) $PdSe_2$. Dots in the shaded area are below the average value.

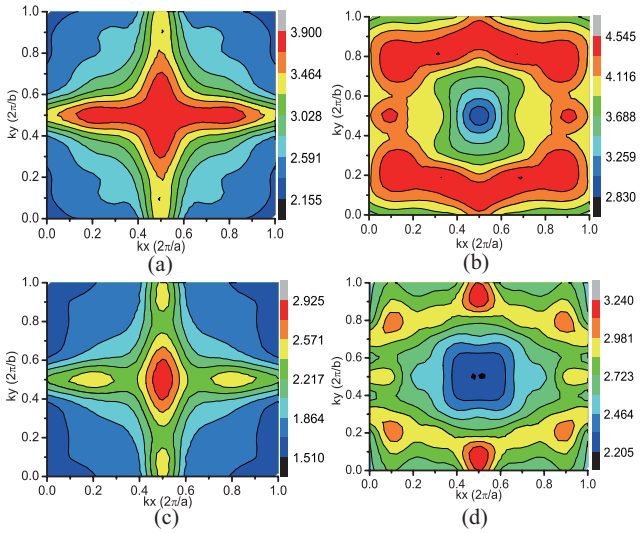

FIG. S8. Contours of the electron-phonon coupling strength for HVB (left column) and LCB (right column) of 3L (a)-(b) and 4L (c)-(d) $PdSe_2$.

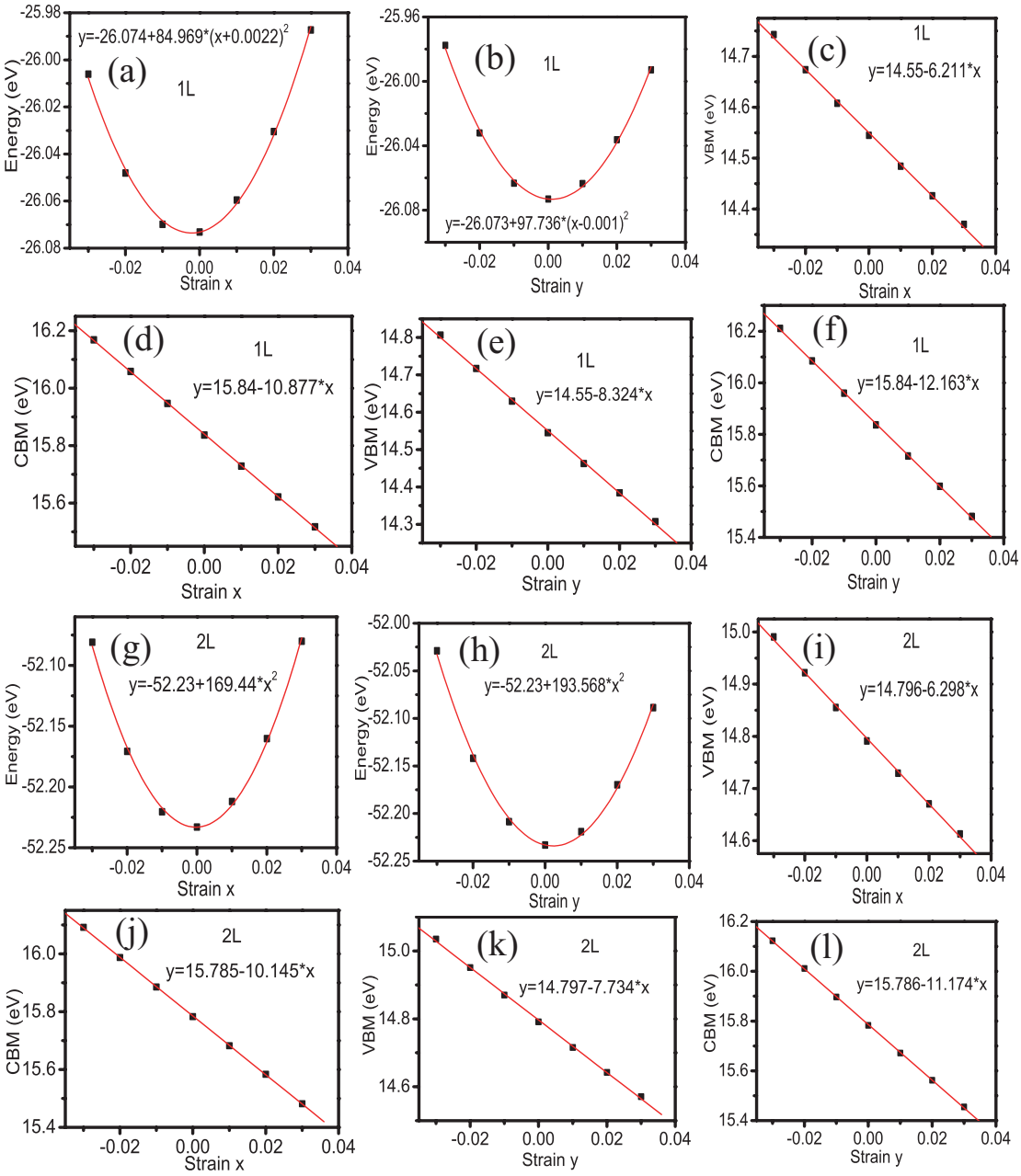

FIG. S9. (a)-(b) Energy variation with respect to the strain for 1L $PdSe_2$. (c)-(f) Elastic constants obtained by fitting the strain -dependent band edge shift for 1L $PdSe_2$. (g)-(h) Energy variation with respect to the strain for 2L $PdSe_2$. (i)-(l) Elastic constants obtained by fitting for 2L $PdSe_2$. The solid lines are the linear fittings.

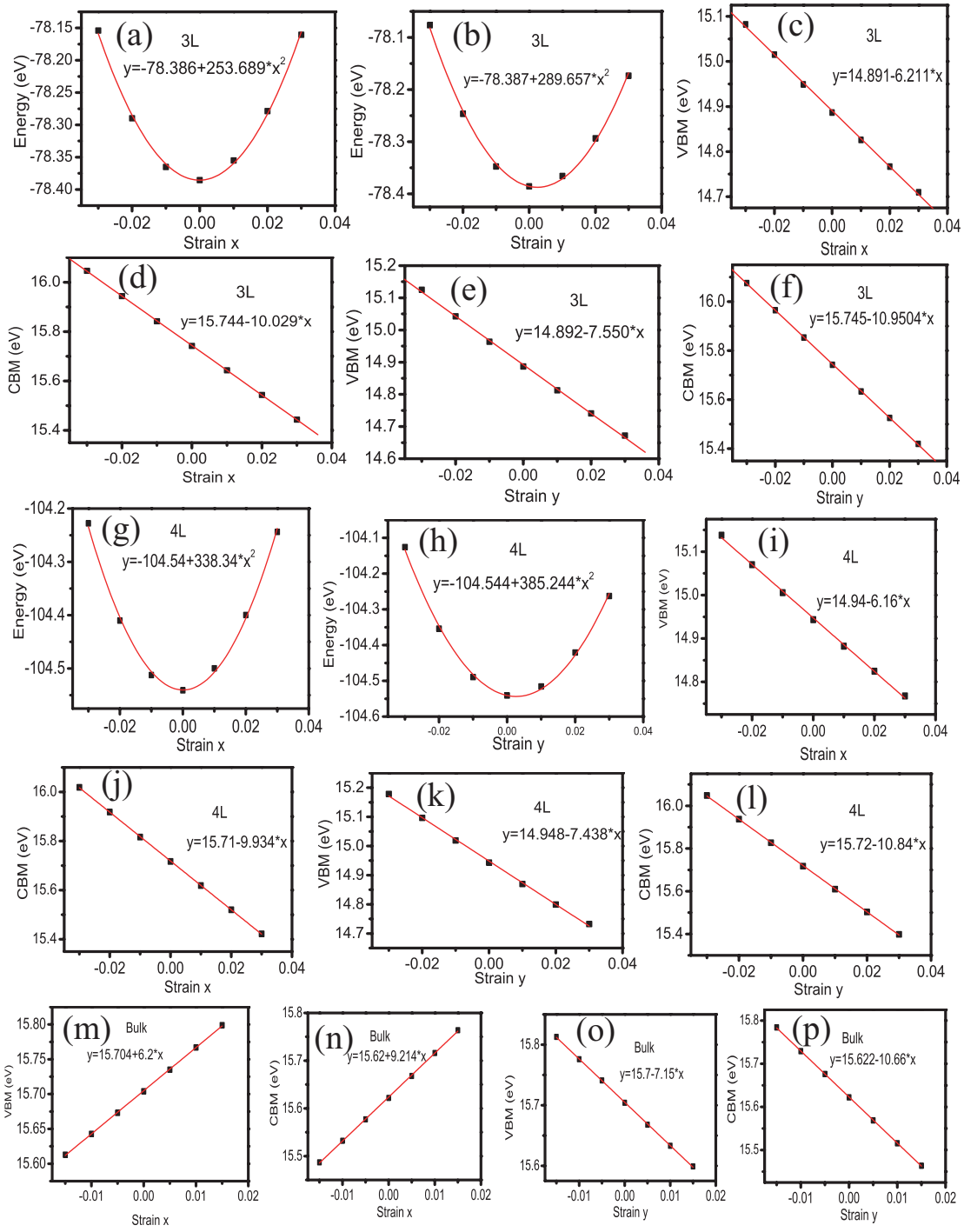

FIG. S10. (a)-(b) Energy variation with respect to the strain for 3L $PdSe_2$. (c)-(f) Elastic constants obtained by fitting the strain -dependent band edge shift for 3L $PdSe_2$. (g)-(h) Energy variation with respect to the strain for 4L $PdSe_2$. (i)-(l) Elastic constants obtained by fitting for 4L $PdSe_2$. (m)-(p) Band edge shift versus the strain. The solid lines are the linear fittings.